

6th CIRP International Conference on High Performance Cutting, HPC2014

Hard broaching of case hardened SAE 5120

Harald Meier^{1*}, Kevin Ninomiya², David Dornfeld² and Volker Schulze¹

¹ *wbk Institute of Production Science, Karlsruhe Institute of Technology (KIT), Kaiserstr. 12, 76131 Karlsruhe, Germany*

² *Laboratory for Manufacturing and Sustainability, University of California, Berkeley, 1115 Etcheverry Hall, Berkeley 94720-1740, United States of America*

* Corresponding author. Tel.: +49-721-608-43044 ; fax: +49-721-608-45005. E-mail address: harald.meier@kit.edu

Abstract

To achieve knowledge of the effects of broaching to the component and the influence on subsequent process steps such as heat treatment and hard machining, broaching experiments were performed on plates made of normalized case hardening steel SAE 5120 in [1]. To investigate the effect of heat treatment, five broaching variants of [1] were chosen and hardened with two different case hardening depths, which were observed for effects generated from the surface layer carbon fraction. The hardened variants were analyzed for distortion generated through the hardening step and the specimen subsequently underwent a hard broaching stage in dry machining conditions. The cutting forces were monitored in-process, and the residual stress of the machined surface was determined using X-ray diffraction after the experiment. Surface roughness measurements also complemented the results. The results indicated that the cutting forces depend on existing distortion and therefore the volume material removed. It can also be seen that there is little influence on cutting forces with rising cutting speeds. Compressive residual stresses were present after heat treatment, but turned into tensile residual stress states after hard broaching. Effects from different case hardening depths and cutting speeds in the formation of surface roughness and residual stress could not be detected.

© 2014 Published by Elsevier B.V. Open access under [CC BY-NC-ND license](https://creativecommons.org/licenses/by-nc-nd/4.0/).

Selection and peer-review under responsibility of the International Scientific Committee of the 6th CIRP International Conference on High Performance Cutting

"Keywords: Machining; Cutting force; Surface roughness; Residual Stress; Optimization; Hard broaching"

1. Introduction

Broaching is a machining process meant for cutting material to desired geometries with high removal rates. A broaching tool is designed with multiple levels of increasing teeth heights throughout the length of the tool. This allows the process to achieve both roughing and finishing processes in a single stroke. A broaching process can already be a standalone process by itself due to its single-stroke production strategy. However, industries often employ a series of manufacturing steps (process chains) in order to meet special specifications required for a product such as hardness, strength or wear resistance, for example. The observed process chains consist of soft broaching, heat treatment and hard broaching before a product is ready for further use or assembly. Information for each process step should be considered individually in order to achieve best results, but it is important to consider the inherent influence and interaction

between each process step to optimize the final product. Soft broaching results were observed in the prequel study [1]. Both dry and wet cutting were tested for the soft broaching experiments with different cutting speeds, tools and coatings, and the influence on process forces and surface integrity such as roughness and residual stress was shown.

Actual research on broaching focuses on simulation of the broaching process, especially on predicting process forces such as Schulze et. al. [2], Ozturk and Budak [3] and Vogel et. al. [4] or on deeper process knowledge in [5-7].

The focus is on hard broaching in order to determine if hard broaching can remove any distortion caused by soft broaching and/or the heat treatment stage for this study. Additionally, the resulting surface integrity after hard broaching is in focus. The hard broaching process parameters were a cutting speed of 60, 80, and 100 m/min. Cutting speed of $v_c = 60$ m/min is the industry standard for a hard broaching process, and two faster cutting speeds were added since [1] showed that faster cutting speeds generally provided better

results based on soft broaching observations. Although it is uncommon to pursue dry cutting during the hard broaching process in industry, dry machining was used for this study to observe similar best-case conditions based on the soft broaching stage results and to provide more information about saving coolant costs in future. Force values were collected in-process while residual stress and distortion values were measured after. X-ray diffraction and surface roughness measurement methods were used. The objective of this study was to observe effects on the surface integrity through the hard broaching stage and determine its relationship with other process parameters while also contributing to the larger picture of broaching process chain optimization.

2. Background and previous work

2.1. Material

From prior research [1], five variants as shown in Fig. 1 were chosen to investigate the effects of heat treatment and subsequent hard broaching (Table 1).

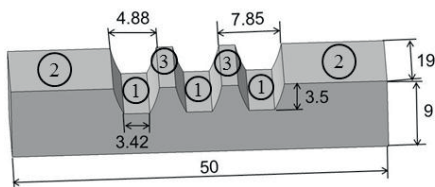


Fig. 1: Geometry of the examined specimen in heat treatment and hard-broaching indicating characteristic measures and surface parts

Table 1: Chosen variants from soft-broaching to perform heat-treatment and hard-broaching experiments

Variant	Cutting speed [m/min]	Rise per tooth [mm]	Lubrication fluid	coating
1	30	0.04	No	TiAlN
2	30	0.06	No	TiAlN
3	50	0.06	Yes	TiAlN
4	7	0.04	No	AlCrN
5	7	0.04	Yes	AlCrN

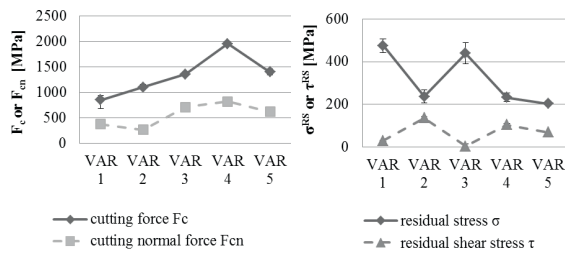


Fig. 2: Overview of cutting (normal) forces (left), residual stress and residual shear stress (right) after soft-broaching for chosen variants [1]

The chosen variants represent the extrema of gained cutting- /cutting normal forces, residual stress and residual shear stress in soft broaching as summarized in Fig. 2.

These variants were intentionally chosen in order to easily observe the effects of soft broaching from [1] and how that may affect the results of the subsequent heat treatment and hard broaching stages which will be described below.

2.2. Heat treatment

The chosen specimen underwent two variants of low pressure carburization at 870 °C for six hours (Variant A) and 11.5 hours (Variant B) with acetylene as carbon donor and a subsequent high pressure nitrogen gas quenching at 10 bars. All specimens showed a martensitic microstructure at the surface with a bainitic core. Two different case hardening depths of CHD = 0.6 HV 0.1 for Variant A and CHD = 0,8 HV 0.1 for Variant B, could be achieved, while a surface hardness of 942 ±12 HV 0.1 was gained. After case hardening, the residual stress state shifted from tensile residual stress towards light compressive residual stress near the surface ($\sigma^{RS} = -200$ MPa) and maximum compressive stress of $\sigma^{RS} = -600$ MPa at a depth of approximately 100 μ m.

2.3. Distortion

Before and after heat treatment, the specimens have been measured using a Zeiss Prismo 5 S-ACC 3-coordinate measuring system. The differences of the measuring point coordinates (between before and after hardening) resulted in a distortion vector. For quantification of the overall distortion within the grooves, the modulus of all distortion vectors was built. The mean value of the vector modulus can be seen as the amount of distortion (Fig. 3).

Additionally, the deflection of the specimen was evaluated. On the upper side of the specimen, the overall surface has been increased by broaching the grooves. By quenching after carburizing, the austenite transforms to martensite which has a higher volume ratio than austenite. This induced a higher elongation of the upper surface parts (Fig. 1, position 1-3) and results in deflection as shown for specimen Variant 3 in Fig. 4. The relative deflection in the grooves (Fig. 1, position 1) was approximately two to three times higher than at the other surface parts (Fig. 1, position 2 and 3). At the grooves, the martensite fraction relative to the total volume is higher than outside the grooves at positions 2 and 3 and therefore the volume change is increased which leads to a higher deflection.

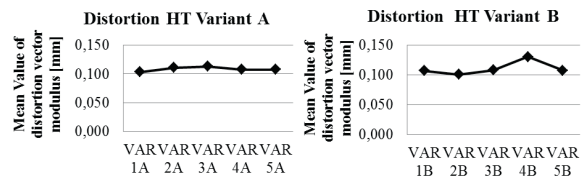


Fig. 3: Mean value of distortion vector modulus for both heat treatment variants

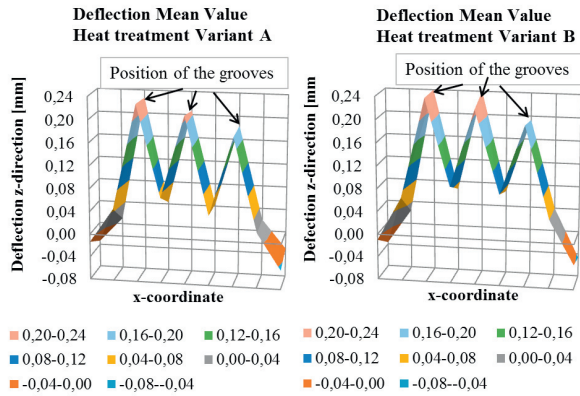


Fig. 4: Deflection after heat treatment in z-direction for Variant 3A (left) and Variant 3B (right)

The maximum deflection mean values in z-direction of all variants are shown in Table 2:

Table 2: maximum deflection mean values for all variants

Variant	Deflection [mm]	Variant	Deflection [mm]
1A	0.22	1B	0.17
2A	0.21	2B	0.19
3A	0.21	3B	0.24
4A	0.11	4B	0.11
5A	0.14	5B	0.14

3. Experimental setup

3.1. Broaching

Broaching experiments were conducted on a broaching machine and using metrology equipment as described in [1]. The broach used was equipped with 3x16 carbide cutting edges and a TiAlN coating with friction coefficient of $\mu = 0.3$. The geometry is given in Fig. 5. For exact positioning of the soft-broached and hardened specimen a fixed stop was integrated in the broach: the specimen fixture positioned the work piece's grooves exactly on the insertion bars (Fig. 5, right, position 1) and was clamped. The first row of broaching teeth (Fig. 5, right, position 2) featured a rise per tooth of $h = 10 \mu\text{m}$ relative to the insertion bars. Subsequent broaching teeth (Fig. 5, right, position 3) had no further rise per tooth and were for cold working and surface smoothing effect, only.

The broaching experiments were performed without lubrication fluid in dry machining with cutting speeds of $v_c = 60, 80$ and 100 m/min .

The deflection of the specimens as shown in Table 2 had negligible influence on the hard broaching process since the grooves were positioned on the insertion bars.

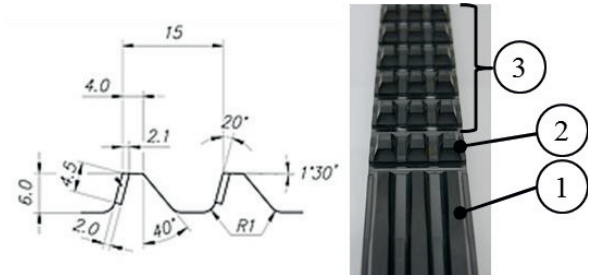


Fig. 5: Broach geometry (left), broaching tool (right)

3.2. Surface roughness

The achieved surface roughness was measured perpendicular to the broaching direction using a stylus instrument type Concept Contour PST-MSE with a stylus type PCV 350-M /59 mm. The scan length was set to 2 mm at a scanning speed of 0.67 mm/sec . A mean value was calculated from six measurements per part, at the tool entrance/emersion side at each groove, respectively.

3.3. Residual Stresses and Cold working

The residual stresses in the ground of the broached groove after hard broaching were analyzed using X-ray stress analysis according to the $\sin^2\psi$ -method [8]. By this means the effect of the broaching parameters on the local residual stress (distribution) near the surface was studied in the middle of the groove. Cr-K α radiation was used to study the $\{211\}$ - α -ferrite diffraction lines at $2\theta_0=156.39^\circ$ for 11 different angles $-45^\circ \leq \psi \leq 45^\circ$. The primary beam was formed using a pin hole collimator with nominal dimension of $\phi = 0.5 \text{ mm}$ and a 4 mm symmetrization slit was used in front of the detector [9]. The interference lines were fitted using a Pearson VII function the X-ray elastic constants $\frac{1}{2}s_2 = 5.82 \cdot 10^{-6} \text{ MPa}^{-1}$ and $s_1 = -1.27 \cdot 10^{-6} \text{ MPa}^{-1}$ were applied for stress calculation.

4. Results

4.1. Cutting forces

The examination of the forces-time plots indicated that the highest forces occur on the first row of teeth, which showed the rise per tooth and is responsible for material removal. After distortion removal, a level of constant forces was set due to tool-work piece friction (Fig. 6). The measured cutting- and cutting normal forces for distortion removal of heat treated variants A in hard-broaching using three different cutting speeds is presented in Fig. 7. Here, the mean value for all teeth has been calculated. As can be seen, the main influence on formation of cutting forces was the fraction material to be removed according to Fig. 3 (left). Therefore, the amount of the cutting speeds chosen had little influence. The spread of the cutting force values was very high and occurred from the different material fraction machined. An examination of the cutting normal forces (Fig. 7, right) revealed, that the lowest cutting speed of $v_c = 60 \text{ m/min}$ tended to be higher than the others. Higher cutting speeds led

to a higher thermal influence in the tool – work piece contact zone and resulted in material softening that decreased cutting forces.

The measured cutting forces for distortion removal of heat treated variants B are given in Fig. 8 (left). As expected, the main influence on force formation was the material fraction to be removed. Again, cutting speed had no observable influence. The evaluation of the cutting normal forces measured by broaching specimens of heat treatment variant B showed no specific trend. Overall, a significant influence of prior machining or variation of heat treatment on formation of distortion with a subsequent influence on hard broaching could not be detected.

To investigate the influence of cutting speed to the formation of cutting- and cutting normal forces, formation of residual stress and cold working, further experiments were conducted. To ensure machining on the tooth root of the grooves, a precision foil was put underneath the upper end of the hard-broach.

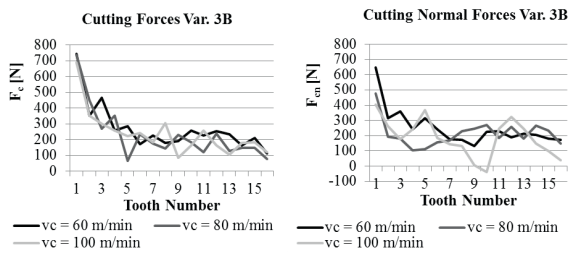


Fig. 6: Formation of forces during one broaching stroke while distortion removal for variant 3B at three different cutting speeds: cutting forces (left) and cutting normal forces (right)

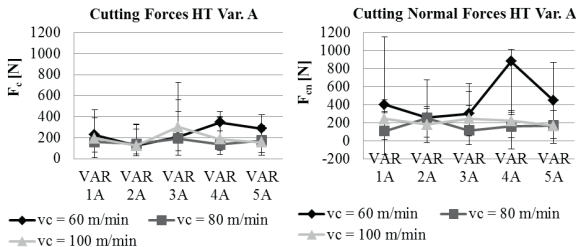


Fig. 7: Cutting forces (left) and cutting normal forces (right) for distortion removal for heat treatment variant A

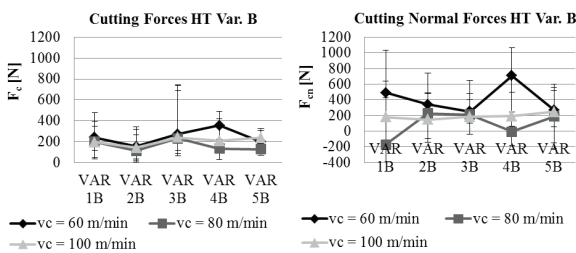


Fig. 8: Cutting forces (left) and cutting normal forces (right) for distortion removal for heat treatment variant B

Therefore, all 3x16 broaching teeth obtain a rise per tooth of $h = 8.75 \mu\text{m}$ and a total depth of cut of $h_{\text{total}} = 140 \mu\text{m}$. This allows the investigation of the cutting forces, surface roughness and resulting residual stress state at profile hard broaching.

The continuous forces plots using the tilted tools in profile hard broaching show, that first more material is removed due to distortion (Fig. 9, left). Highest forces at tool entry of $F_c = 1297 \text{ N}$ were achieved with a cutting speed of $v_c = 80 \text{ m/min}$, lowest forces of $F_c = 942 \text{ N}$ occurred at a cutting speed of $v_c = 100 \text{ m/min}$. The lowest cutting speed of $v_c = 60 \text{ m/min}$ showed cutting forces of $F_c = 1052 \text{ N}$. Once the plus material is removed, a lower, constant level of cutting forces is set indicating chipping a constant material portion. With further progress, the cutting section due to the profile is increased and therefore the cutting forces increase. As can be seen, an influence of the cutting speed applied is not given. Again, lower cutting temperatures when using the low cutting speed of $v_c = 60 \text{ m/min}$ lead to less material softening in the shear zone and therefore to higher cutting normal forces (Fig. 9, right).

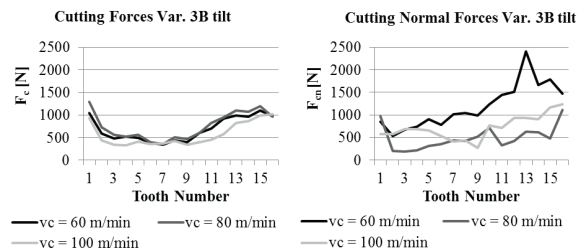


Fig. 9: Formation of forces during one broaching stroke using the tilted tool for variant 3B at three different cutting speeds: cutting forces (left) and cutting normal forces (right)

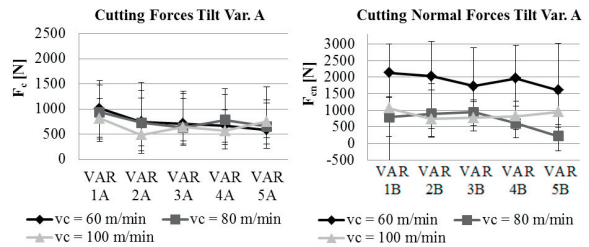


Fig. 10: Cutting Forces (left) and cutting normal forces (right) for Profile Hard Broaching machining specimens of heat treatment variant A

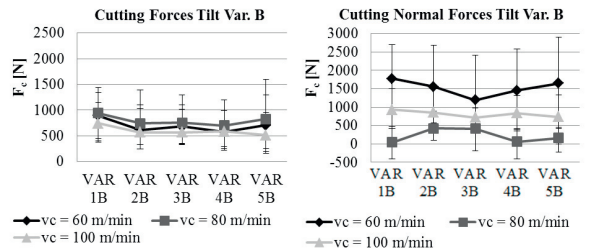


Fig. 11: Cutting Forces (left) and cutting normal forces (right) for Profile Hard Broaching machining specimens of heat treatment variant B

The overview of the cutting (normal) forces by calculating the mean value over all teeth and using the tilted broaching tool for heat treatment variant A is given in Fig. 10. The cutting forces (Fig. 10, left) show no dependency of the cutting speed. The forces measured are located between 500 - 1000 N. The same results were achieved broaching specimens of heat treatment variant B (Fig. 11, left). As described before, an influence of the cutting speed to the cutting normal forces can be detected for both hardening variants A and B (Fig. 10, right; Fig. 11, right). The low cutting speed of $v_c = 60$ m/min leads to the highest normal forces in each case. Applying higher cutting speeds, the trend is not clear: for heat treatment variants A no influence can be detected, the force values oscillate around 1000 N, whereas at variants B the cutting normal forces measured at a cutting speed of $v_c = 80$ m/min are clearly smaller. This phenomenon cannot be explained.

4.2. Surface Roughness

Fig. 12 shows the measured surface roughness after hard broaching for all variants and cutting speeds. For heat treatment variants A and B, a consolidated mean value was found since there was no significant difference between both variants. An influence of cutting speed to the formation of surface roughness could not be detected. A smooth, reflecting surface for all components could be detected. Furthermore, all specimens show values in the range of $R_a = 0.4 \mu\text{m}$, what stands for a reduction of roughness by a factor 5 compared to soft broaching results shown in [1].

4.3. Residual Stresses and Cold working

After hard broaching with the tilted tool, residual stress depth profiles were measured at the tooth root surface of the middle groove as shown in Fig. 13. It can be seen, that the stress profile changed to tensile residual stress compared to after heat treatment. The residual stress at the surface reaches values of $\sigma^{RS} = 547 - 630$ MPa, maximum tensile stresses of $\sigma^{RS} = 663 - 814$ MPa were detected beneath the surface at a depth of $25 \mu\text{m}$.

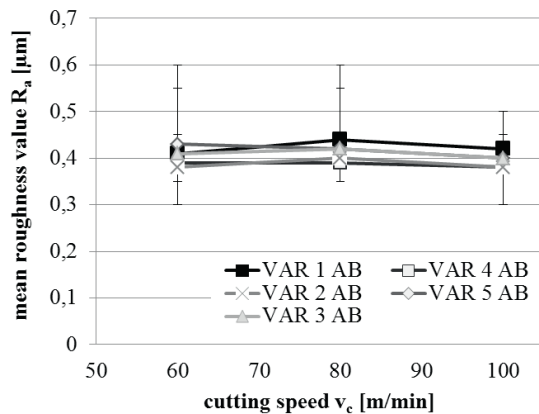


Fig. 12: Measured surface roughness on the hard broached surface for varied cutting speeds v_c and both heat treatment variants A and B

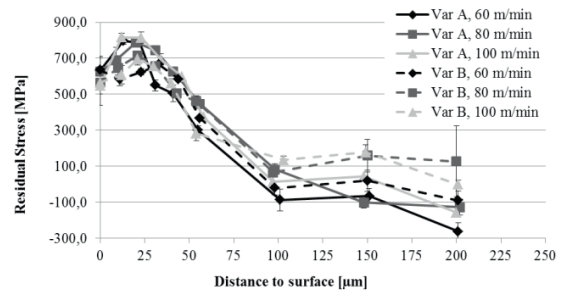


Fig. 13: Measured residual stress depth profiles on the hard broached specimens for varied cutting speeds v_c and both heat treatment variants A and B

Subsequently, the tensile stresses decrease with increasing component depth and reach levels of $\sigma^{RS} = \pm 0$ MPa at a depth of $100 \mu\text{m}$. This corresponds to values directly after case-hardening. The highest tensile residual stresses were generated with specimen from heat treatment A and a cutting speed of $v_c = 100$ m/min featuring $\sigma^{RS} = 547$ MPa at the surface and $\sigma^{RS} = 814$ MPa at a depth of $24 \mu\text{m}$. The lowest tensile residual stresses were generated with specimen from heat treatment B and a cutting speed of $v_c = 60$ m/min featuring $\sigma^{RS} = 563$ MPa at the surface and $\sigma^{RS} = 664$ MPa at a depth of $33 \mu\text{m}$. Overall, there is no significant influence of the previous variant of heat treatment nor an influence of the cutting speed applied detectable. Effects of increasing temperatures and therefore higher tensile residual stresses due to higher cutting speeds are contrary to expectations not visible.

The effect of dry hard broaching on the local strain hardening of the machined surface was determined by conducting a full width on half maximum (FWHM) analysis on the broached tooth root surface. The FWHM is a measure correlated to the degree of cold working: as dislocation density of plastically deformed surface layers increases, the FWHM increases. This can be evaluated by analyzing the resultant X-ray interference patterns.

Fig. 14 shows the measured FWHM of all broached specimen machined with three different cutting speeds on both heat treatment variants. After carburizing and quenching, a high dislocation density is present which is represented by high FWHM values of up to 8° . By initiating the broaching process that goes along with plastically deformation and annealing due to the process temperatures from chip removal, the dislocations are rearranged and partially annihilated and leads to lower FWHM-values as presented in Fig. 14. The mechanically induced part of this effect has also been detected from Burgahn et.al. [10] while shot peening SAE4140 -steel. Directly on the surface, values of $\text{FWHM} = 5-6^\circ$ were achieved, reaching their minimum at a depth of $10 \mu\text{m}$. This implies, that by hard broaching along with introduced chip removal heat rearrangements of dislocations and annealing are initiated. The increase of FWHM at the outer surface layer can be traced back to plastic deformation of the material cut.

Again, it turns out, that neither case hardening depth nor the cutting speed applied has an influence on work hardening.

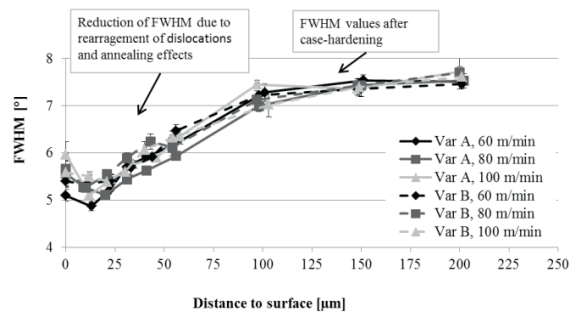


Fig. 14: Measured full width at half maximum (FWHM) on the hard broached specimens for varied cutting speeds v_c and both heat treatment variants A and B

5. Conclusion

The main objective of the study was to observe for effects from the previous soft broaching work presented in [1]. In this study, it was shown that after case hardening, the former influences of soft broaching were equalized. A convex distortion of the specimen was detected, which is due to formation of martensite and therefore an increase of volume of the upper surface parts. A higher case hardening depth does not lead to more distortion. After case hardening, compressive residual stresses were found as expected. When accomplishing a hard broaching process for distortion removal, the occurring cutting forces depended on the material fraction removed. In profile hard broaching, no influence of the cutting speed on the formation of cutting forces could be found, whereas lower cutting speeds led to higher cutting normal forces. After hard broaching, the residual stress state turned from compressive residual stress to tensile residual stress due to heat influence from the machining process. The surface roughness was decreased by a factor 5 compared to the results in soft broaching.

Regarding the complete process chain “soft broaching – case hardening – hard broaching”, it can be stated that the previous broaching process of normalized steel had no further influence to subsequent manufacturing steps. Here, the broaching process can be designed on the basis of economic criteria: to realize short process times, the cutting speed can be increased what leads, on one hand, to decreasing cutting forces and on the other hand to less tool wear as described by [11]. A further increase of the rise per tooth leads to shorter broaching tools which save acquisition- and regrinding costs.

After hard broaching, the previous, advantageous compressive residual stresses are changed to tensile residual stresses, which may lead to problems when cyclic loads are applied. Here, research has to be continued to apply more deformation/ cold working within the broaching stroke to gain compressive residual stress states. While hardened specimens feature little plasticity, special care especially at inner broaching should be taken, otherwise fatal component breakage can occur due to high normal forces.

Dry hard broaching promises high competition benefits since it is a high productive finishing process which can improve tolerances and surface roughness for difficult-to-machine geometries such as those present in inner gears.

Acknowledgements

The authors would like to thank IWT Bremen for performing case hardening, the Institute of Applied Materials IAM-WK for residual stress measurements. Further, we gratefully acknowledge the financial support of the German research foundation (DFG) within the Research Training Group 1483 “Process Chains in Production: Interaction, Modeling, and Assessment of Process Zones”. Additional gratitude goes to the German Academic Exchange Service (DAAD) for enabling the research exchange within the RISE-program.

References

- [1] Schulze, V.; Meier, H.; Strauss, T.; Gibmeier, J.: High Speed Broaching of Case Hardening Steel SAE 5120. 5th CIRP International Conference on High Performance Cutting. Procedia CIRP 1;2012; p. 431-436
- [2] Schulze, V.; Boev, N.; Zanger, F.: Numerical investigation of the changing cutting force caused by the effects of process machine interaction while broaching. 3rd CIRP Conference on Process Machine Interaction, Procedia CIRP 4;2012; p. 139-144
- [3] Ozturk Budak: Modeling of broaching process for improved tool design. Proceedings of IMECE'03, 2003 ASME International Mechanical Engineering Congress & Exposition; 2003; p. 1-11
- [4] Vogel, P.; Klocke, F.; Puls, H.; Buchkremer, S.; Lung, D.: Modelling of process forces in broaching Inconel 718. 14th CIRP Conference on Modeling of Machining Operations (CIRP CMMO), 2013; p. 409-414
- [5] Schulze, V.; Zanger, F.; Boev, N.: Numerical Investigations on Changes of the Main Shear Plane while Broaching. 14th CIRP Conference on Modeling of Machining Operations (CIRP CMMO), Procedia CIRP 8; 2013; p. 245-250.
- [6] Schulze, V.; Osterried, J.; Strauß, T.: FE analysis on the influence of sequential cuts on component conditions for different machining strategies. 1st CIRP Conference on Surface Integrity (CSI); 2012; p. 318-323.
- [7] Schulze, V.; Osterried, J.; Strauß, T.; Zanger, F.: Analysis of surface layer characteristics for sequential cutting operations. HTM Journal of heat treatment and materials; Volume 67; 2012; p. 347-356.
- [8] Macherauch E, Müller P. Das $\sin^2\psi$ -Verfahren der röntgenographischen Spannungsmessung. Z. angew. Physik, 13; 1961; p. 305-312.
- [9] Wolfstieg U. Die Symmetrisierung unsymmetrischer Interferenzlinien mit Hilfe von Spezialblenden, HTM 31; 1976; p. 23-26.
- [10] Burgahn F.; Vöhringer O.; Macherauch E.: Mikroeigenzustände kugelgestrahlter Randschichten von 42 CrMo 4, Zeitschrift für Metallkunde 84; 1994; p. 224-229.
- [11] Meier H, Rilli R, Schulze V. Nass- und Trockenräumen von 16MnCr5. Proceedings of Research Training Group 1483 and CCMSE, 2010; p. 39-43